

Electrically tunable dielectric properties of Ba_{0.6}Sr_{0.4}TiO₃-MgO composite ceramics

Xiao-Fei Zhang^{a,b}, Qing Xu^{b,*}, Di Zhan^b, Bok-Hee Kim^{c,*}, Kai Zhao^c and Duna-Ping Huang^b

^aSchool of Mathematics and Physics, Hubei Polytechnic University, Huangshi 435003, People's Republic of China

^bSchool of Materials Science and Engineering, Wuhan University of Technology, Wuhan 430070, People's Republic of China

^cDivision of Advanced Materials Engineering, Hydrogen & Fuel Cell Research Center, Chonbuk National University, Jeonju 561-756, Republic of Korea

40 wt.% Ba_{0.6}Sr_{0.4}TiO₃-60 wt.% MgO composite ceramics were prepared from Ba_{0.6}Sr_{0.4}TiO₃ powder synthesized by a citrate method and fine MgO powder. The composite ceramics sintered at 1150-1270 °C attained reasonable densification. The structure and dielectric properties of the specimens were investigated. The results showed an important role of sintering temperature in controlling the microstructure and dielectric properties of the specimens. Sintering at 1250 °C was determined to be preferred in terms of the nonlinear dielectric properties of the specimens under bias electric field. The specimen sintered at 1250 °C attained a dielectric constant (ϵ_r) of 207 and a dielectric loss ($\tan\delta$) of 0.11% at 10 kHz together with a tunability of 18.5% and a figure of merit (FOM) of 168 at 10 kHz and 30 kV/cm. It was found that the nonlinear dielectric properties of the specimen measured in continuous cycles of bias electric field sweep were dependent on field history. The phenomenon is qualitatively explained in relation to the polarization reorientation of polar nano-regions (PNRs) in Ba_{0.6}Sr_{0.4}TiO₃ phase of the composite specimen.

Key words: Ba_{0.6}Sr_{0.4}TiO₃-MgO, Composite ceramics, Nonlinear dielectric properties, Microstructure.

Introduction

Barium strontium titanate (Ba_{1-x}Sr_xTiO₃, BST) exhibits strong dielectric nonlinearity under bias electric field and adjustable Curie temperature. The desired properties make BST a promising candidate material for electrically tunable microwave dielectric devices. Along with high tunability, it is desired that the dielectric materials for the tunable microwave devices have a moderate dielectric constant to achieve good impedance matching and a low dielectric loss to reduce the overall insertion loss. In this sense, large dielectric constants and relatively high dielectric losses of BST compositions are unfavorable for the tunable device applications. Adopting composite design comprising BST and non-ferroelectric components was recognized as an effective strategy to tailor the dielectric parameters [1-3]. To this aim, MgO [4, 5] and magnesium-containing complex oxides, such as Mg₂SiO₄ [6, 7], Mg₂TiO₄ [8], MgAl₂O₄ [9, 10] and MgTiO₃ [11], were employed as the non-ferroelectric components. The dielectric properties of BST-based composites were unraveled in terms of doping effect and composite mixing effect [5]. Some BST-based composites showed dielectric behaviors different from BST, such as relaxor-like behavior, which were explained with respect to the change in crystal structure and

microstructure with the addition of the non-ferroelectric components [8-11]. It was demonstrated that the nonlinear dielectric properties of the composites were highly dependent on microstructure and closely related with the peculiarities of added non-ferroelectric components [6, 7].

From a microstructure viewpoint, BST-based composites comprise more than one constituent disparate in dielectric nature. The nonlinear dielectric properties of the composites essentially are determined by the response of involved polarization mechanisms under applied bias electric field. Studying the dielectric response of the composites under bias electric field would offer critical information of the polarization mechanisms. A deep insight into the issue might be favorable for better understanding the contribution of various constituents to the dielectric nonlinearity and in turn guiding the design of new composites with desirable properties [7]. On the other hand, BST-based composites suffer from high sintering temperatures (> 1350 °C). It is expected that lowering sintering temperature would leave a larger space for the realization of the dielectric composites in the tunable microwave devices [12, 13].

We prepared Ba_{0.6}Sr_{0.4}TiO₃ ceramics with reasonable densification (near 95% of the theoretical density) at sintering temperature of 1260 °C by using superfine power derived from a citrate method [14]. The dielectric response of the ceramics under bias electric field was investigated [15]. As a consecutive effort, we prepared Ba_{0.6}Sr_{0.4}TiO₃-MgO composite ceramics from fine starting powders at sintering temperatures of 1150-1300 °C. In this work, we inspect the nonlinear

*Corresponding author:

Tel : +86-27-87863277 ; +82-63-270-2380

Fax: +86-27-87864580 ; +82-63-270-2386

E-mail: xuqing@whut.edu.cn ; kimbh@jbnu.ac.kr

dielectric properties of the composite ceramics under bias electric field.

Experimental

$Ba_{0.6}Sr_{0.4}TiO_3$ powder was synthesized by a citrate method using reagent grade $Ba(NO_3)_2$, $Sr(NO_3)_2$, tetrabutyl titanate and citric acid as starting materials. Citric acid was dissolved in deionized water. After adjusting the pH value of the solution to 7-9, tetrabutyl titanate, $Ba(NO_3)_2$ and $Sr(NO_3)_2$ were added under stirring to form a transparent aqueous solution. The precursor solution was heated at 300 °C to form a foam-like solid precursor. The foam precursor was pulverized and calcined at 550 °C. The calcined powder showed a single perovskite phase and superfine particle morphology (100 nm). The synthesis and characterization of the powder have been reported elsewhere [14]. The composite ceramics with the nominal composition of 40 wt.% $Ba_{0.6}Sr_{0.4}TiO_3$ -60 wt.% MgO were prepared from the $Ba_{0.6}Sr_{0.4}TiO_3$ powder and commercial MgO powder (99.9%, Nanjing High Technology Nano Material Co., Ltd.). The Brunauer-Emmett-Teller (BET) measurement of MgO powder indicated a specific surface area of 11.2 m²/g and a mean particle size of 150 nm. The two starting powders were thoroughly mixed and then uniaxially pressed into discs of 13 mm in diameter and 1 mm in thickness under a pressure of 300 MPa. The compacted discs were sintered at 1150-1300 °C for 2 h in air. For comparison purposes, $Ba_{0.6}Sr_{0.4}TiO_3$ ceramics were produced at sintering temperature of 1260 °C.

The X-ray diffraction (XRD, Philips X'pert PBO X-ray diffractometer using Cu K α radiation) analysis of the specimens was performed. The microstructure of the specimens was investigated using polished and thermally-etched surfaces using a scanning electron microscope (SEM, Jeol JSM-5610LV attached with an energy dispersive spectroscopy (EDS) analyzer). The grain size of the specimens was estimated by image analysis using the Image-Pro Plus 6.0 software. The bulk density of the specimens was measured by the Archimedes method with ethyl alcohol as medium. The theoretical density of the specimens was calculated according to the mixing rule. The relative densities were determined from the measured and calculated data.

The specimens were polished and painted with silver paste on both surfaces as electrodes. The temperature dependence of the dielectric constant (ϵ_r) was measured by a TH2828 precision LCR meter (20 Hz-1 MHz) and a SSC-M10 environmental chamber (C4 controller) between -70 and 110 °C. The nonlinear dielectric properties under bias electric field were measured at room temperature by a TH2818 automatic component analyzer at 10 kHz. A blocking circuit was adopted to protect the analyzer from applied high bias voltages. The dielectric properties were measured in continuous cycles of bias

electric field sweep. In each cycle, bias electric fields were forward swept in steps of 1 kV/cm from 0 to 30 kV/cm and then backward swept to 0 kV/cm. Dielectric data were recorded after holding at each applied field for 10 sec. The measurement was continuously performed for 8 cycles.

Results and Discussion

Structural evolution with sintering temperature

Fig. 1 shows the XRD patterns of $Ba_{0.6}Sr_{0.4}TiO_3$ specimen and the composite specimens sintered at different temperatures. $Ba_{0.6}Sr_{0.4}TiO_3$ specimen had a cubic perovskite structure, while the composite specimens presented a biphasic structure comprising a cubic $Ba_{0.6}Sr_{0.4}TiO_3$ phase and a cubic MgO phase. The result suggests that the chemical reaction between the two constituent phases during sintering appears to be insignificant. Compared with $Ba_{0.6}Sr_{0.4}TiO_3$ specimen, the XRD peaks of $Ba_{0.6}Sr_{0.4}TiO_3$ phase in the composite specimens slightly shifted towards higher diffraction angle directions. The phenomenon is attributed to the generation of oxygen vacancies stemming from the substitution of Mg^{2+} for Ti^{4+} [5]. The peak shift implies a reduction of the unit cells in dimension for $Ba_{0.6}Sr_{0.4}TiO_3$ phase of the composite specimens as compared to $Ba_{0.6}Sr_{0.4}TiO_3$ specimen. For the composite specimens, the peak positions of $Ba_{0.6}Sr_{0.4}TiO_3$ phase basically retained invariant whatever the sintering temperatures.

Fig. 2 shows the relative densities of the composite specimens as a function of sintering temperature. The relative densities increased with sintering temperature through a maximum value at 1250 °C and then decreased. For the composite specimens, the sintering temperatures required for achieving reasonable densification were much lowered as compared with the case of BST-MgO composite ceramics prepared by the conventional method [5]. The improved sintering property of the specimens is ascribed to high activity of the fine starting powders. The

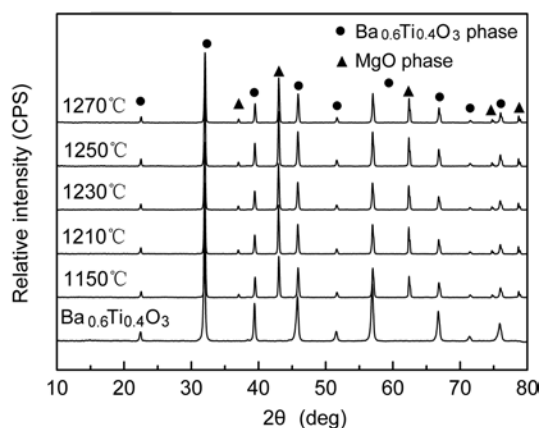


Fig. 1. XRD patterns of $Ba_{0.6}Sr_{0.4}TiO_3$ specimen sintered at 1260 °C and the composite specimen sintered at different temperatures.

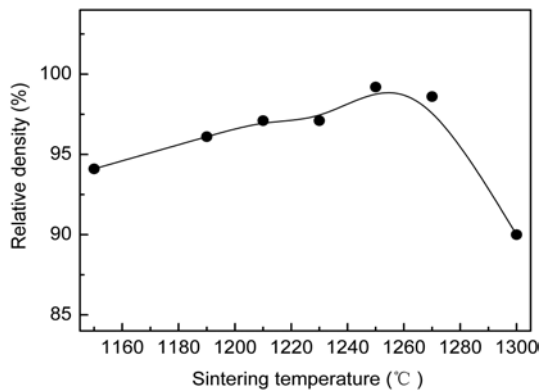


Fig. 2. Relative density of the composite specimens as a function of sintering temperature.

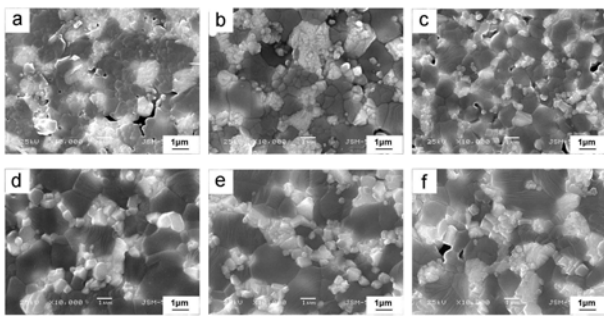


Fig. 3. SEM images of the composite specimens sintered at (a) 1150, (b) 1190, (c) 1210, (d) 1230, (e) 1250 and (f) 1270 °C.

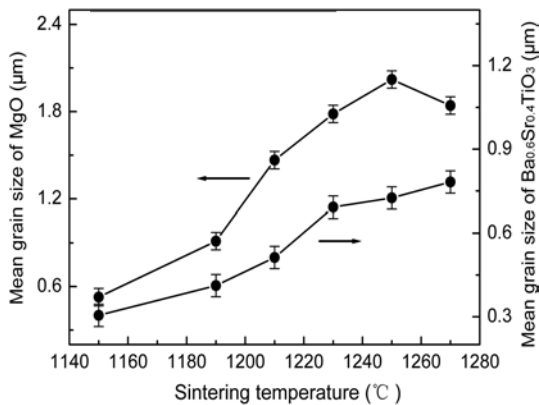


Fig. 4. Mean grain sizes of Ba_{0.6}Sr_{0.4}TiO₃ and MgO phases as a function of the sintering temperature of the composite specimens.

relative density of the composite specimen sintered at 1300 °C apparently declined to about 90%. We excluded the specimen from the subsequent inspection due to its unsatisfactory densification.

Fig. 3 shows the SEM images of the composite specimens sintered at different temperatures. Two sorts of grains distinct in contrast and size were observed. The EDS analysis indicated that the light and relatively small grains correspond to Ba_{0.6}Sr_{0.4}TiO₃ phase while the dark and relatively large ones MgO phase, consistent with previous result [16]. The evolution of microstructure with sintering temperature is in good

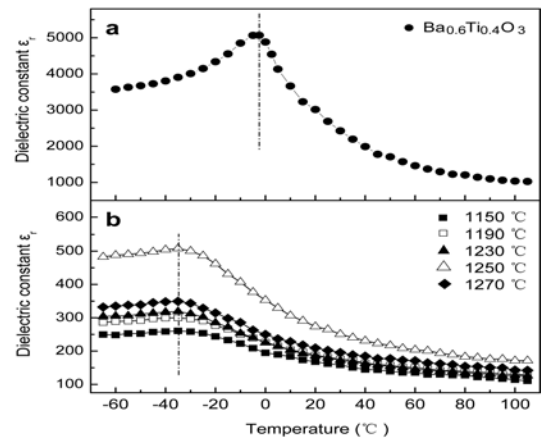


Fig. 5. Temperature dependence of the dielectric constant (ϵ_r) measured at 10 kHz for (a) Ba_{0.6}Sr_{0.4}TiO₃ specimen sintered at 1260 °C and (b) the composite specimens sintered at different temperatures.

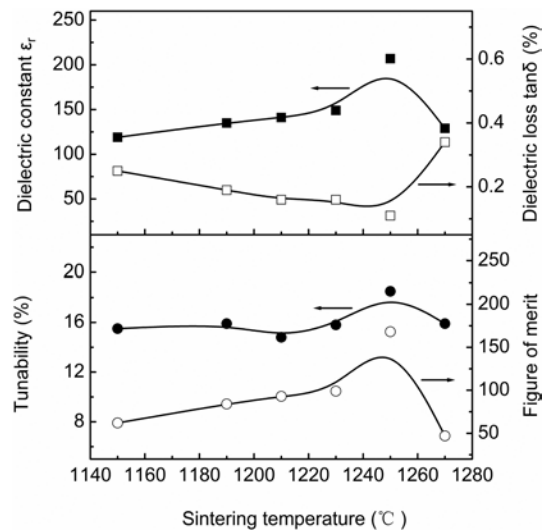


Fig. 6. Nonlinear dielectric properties of the composite specimens sintered at different temperatures.

agreement with that of the relative density (Fig. 2). Moreover, the grains of Ba_{0.6}Sr_{0.4}TiO₃ phase maintained a good percolation. Fig. 4 shows the mean grain sizes of Ba_{0.6}Sr_{0.4}TiO₃ and MgO phases in the composite specimens. On increasing sintering temperature, the grains of both phases tended to be larger.

Effect of sintering temperature on dielectric properties

Fig. 5 shows the temperature dependence of the dielectric constant (ϵ_r) measured at 10 kHz for Ba_{0.6}Sr_{0.4}TiO₃ specimen and the composite specimens sintered at different temperatures. The dielectric constant of Ba_{0.6}Sr_{0.4}TiO₃ specimen displayed a diffuse peak at around -2.5 °C (Fig. 5(a)), which is consistent with previous result [17]. The dielectric anomaly, as well known, is attributed to a ferroelectric-paraelectric phase transition. The composite specimens provided an

analogous dielectric behavior (Fig. 5(b)). Compared with $Ba_{0.6}Sr_{0.4}TiO_3$ specimen, the dielectric constant peaks of the composite specimens were apparently depressed and broadened. This change is due to the mixing effect of MgO as a non-polar constituent of the composite system [5]. Meanwhile, the temperature for the maximum of the dielectric constant (T_m) moved to -35°C for the composite specimens. The T_m movement is assigned to the effect of Mg^{2+} doping into the lattice of $Ba_{0.6}Sr_{0.4}TiO_3$ phase [18]. The T_m value (-35°C) of the composite specimens suggests a macroscopically paraelectric state for $Ba_{0.6}Sr_{0.4}TiO_3$ phase at room temperature, coinciding with the result of the XRD analysis (Fig. 1).

Fig. 6 shows the nonlinear dielectric properties of the composite ceramics sintered at different temperatures. The dielectric constant (ϵ_r) and the loss ($\tan\delta$) were measured at zero bias field. As the percentage of dielectric constant change at 30 kV/cm, the tunability was determined from the data measured in forward bias field sweep of the first cycle. The figure of merit (FOM, defined as $\text{tunability}/\tan\delta$) was calculated from the tunability and the dielectric loss. One can see a significant effect of sintering temperature on the nonlinear dielectric parameters. This effect can be qualitatively interpreted with respect to the evolution of the densification and microstructure with sintering temperature. The densification development of the specimens (Figs. 3(a-e)) and grain growth of $Ba_{0.6}Sr_{0.4}TiO_3$ phase (Fig. 4) with increasing sintering temperature are favorable for enhancing the dielectric constant. On the other hand, the appearance of micropores at 1270°C (Fig. 3(f)) resulted in a deleterious effect. As a result, the maximum value of the dielectric constant occurred at 1250°C . The variation of the dielectric loss with sintering temperature can be easily understood in view of the evolution of the densification (Fig. 2 and Fig. 3).

The tunability afforded a variation with sintering temperature identical to that of the dielectric constant. This identity is rational on account of the correlation of the two dielectric parameters in physics [19]. As the definition indicates, the FOM relies on the trade-off of the tunability and the dielectric loss, with the specimen sintered at 1250°C achieving the largest value. The FOM has been viewed as a criterion to evaluate the overall property of nonlinear dielectrics [17]. According to the criterion, sintering at 1250°C was determined to be preferred for the composite ceramics.

Dependence of nonlinear dielectric properties on history of applied bias electric field

Fig. 7 shows the dielectric constants measured in different cycles of bias electric field sweep for the composite specimen sintered at 1250°C . For each sweep, the dielectric constant of the specimen steadily declined with the increase of applied bias electric field in magnitude. Considering the nature of MgO as a non-

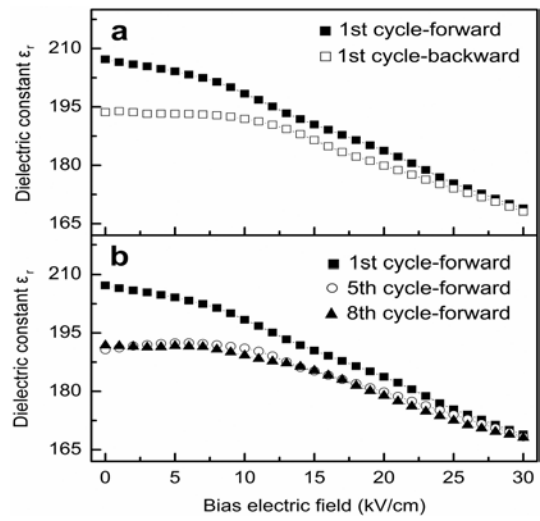


Fig. 7. Dielectric constants measured in different cycles of bias electric field sweep for the composite specimen sintered at 1250°C .

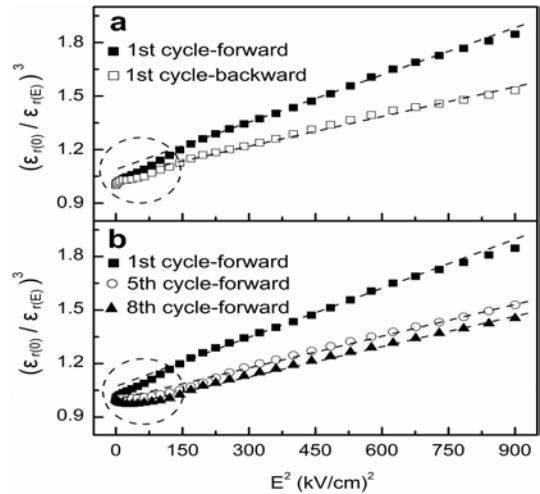


Fig. 8. The $(\epsilon_{r(0)}/\epsilon_{r(E)})^3$ vs. E^2 plots of the composite specimens sintered at 1250°C . The dielectric constants were measured in different cycles of bias electric field sweep. The dashed lines illustrate a linear relation. The dashed circles illustrate the deviation of the measured data from the framework as predicted by the Johnson relation.

polar dielectric, it is believed that the dielectric nonlinearity of the composite specimen is assignable to $Ba_{0.6}Sr_{0.4}TiO_3$ phase. Moreover, the nonlinear dielectric response of the specimen under bias electric field was sensitive to field history. This result is analogous to the behavior of the $Ba_{0.6}Sr_{0.4}TiO_3$ ceramics, which was related to the presence of polar nano-regions (PNRs) embedded in the macroscopically paraelectric background of the ceramics [15, 20].

The dielectric constants measured under bias electric field were fitted to the Johnson's phenomenological relation, as described by the following equation [21]:

$$\frac{\epsilon_r(E)}{\epsilon_r(0)} = \frac{1}{[1 + \alpha\epsilon_0^3\epsilon_r(0)^3E^2]^{1/3}} \quad (1)$$

where ϵ_0 is the permittivity of free space, $\epsilon_r(E)$ and $\epsilon_r(0)$

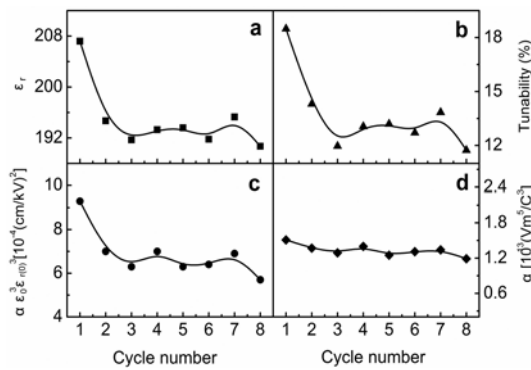


Fig. 9. Parameters of dielectric nonlinearity as a function of cycle number for the composite specimen sintered at 1250 °C. The parameters were derived from the experimental data measured in forward bias electric field sweeps.

represent the dielectric constants under a bias field and zero bias field, respectively, and α is the anharmonic coefficient. The pre-factor term of E^2 , $\alpha\epsilon_0^3\epsilon_{r(0)}^3$, is defined as the field coefficient, quantifying the efficiency of applied bias field in depressing dielectric constant [22]. Figure 8 shows the $(\epsilon_{r(0)}/\epsilon_{r(E)})^2$ vs. E^2 plots of the composite specimen sintered at 1250 °C. The dielectric constants were measured in different cycles of bias electric field sweep. For each sweep, the measured data roughly agreed with the behavior as predicted by the phenomenological expression (i.e. a linear relation). The Johnson relation is intended to depict the dielectric constant under bias electric field for polar dielectrics in paraelectric state [20, 21]. In this context, the rough agreement of the measured data with the Johnson relation should be associated with the good percolation of the grains of $\text{Ba}_{0.6}\text{Sr}_{0.4}\text{TiO}_3$ phase (Fig. 3).

At a closer look, the measured data slightly deviated from the Johnson framework at bias fields below ~12 kV/cm. The deviation can be attributed to polarization reorientation of PNRs in $\text{Ba}_{0.6}\text{Sr}_{0.4}\text{TiO}_3$ phase under bias electric field. Similar phenomenon was observed for $\text{Ba}_{0.6}\text{Sr}_{0.4}\text{TiO}_3$ specimen, with a deviation occurring at lower bias fields (<~5 kV/cm) [15]. The difference in the deviation behavior between $\text{Ba}_{0.6}\text{Sr}_{0.4}\text{TiO}_3$ specimen and the composite specimen can be explicated in view of a field-distribution effect. The biphasic structure of the composite specimen means a distribution of applied bias electric field between the two phases [23]. Considering disparate dielectric features of the two phases, it is plausible that the bias field practically applied on polar $\text{Ba}_{0.6}\text{Sr}_{0.4}\text{TiO}_3$ phase accounts for a minor part. This occurrence is presumed to be responsible for the different deviation behaviors of $\text{Ba}_{0.6}\text{Sr}_{0.4}\text{TiO}_3$ specimen and the composite specimen.

Fig. 9 shows the parameters of the dielectric nonlinearity as a function of cycle number for the composite specimen sintered at 1250 °C. The parameters

were derived from the experimental data measured in forward bias field sweeps. The dielectric constant, tunability and field coefficient offered an identical variation, apparently dropping with increasing cycle number in the first three cycles and then fluctuating (Figs. 9a, b and c). This result is similar to that of $\text{Ba}_{0.6}\text{Sr}_{0.4}\text{TiO}_3$ specimen [15], embodying a field history dependence of the dielectric nonlinearity. Unlike the case of the three parameters, the anharmonic coefficient basically was independent of cycle number (Fig. 9d). The independence is logical because the parameter essentially is related with the intrinsic polarization mechanism (i.e. lattice phonon polarization) of $\text{Ba}_{0.6}\text{Sr}_{0.4}\text{TiO}_3$ phase [20, 21, 24]. The independent behavior of the anharmonic coefficient in turn indicates that the field history dependence of the dielectric nonlinearity should be related with extrinsic polarizable species.

Bias field-induced polarization freezing of PNRs in $\text{Ba}_{0.6}\text{Sr}_{0.4}\text{TiO}_3$ phase is proposed to be the scenario to explain the degradation of the dielectric nonlinearity with cycle number. The PNRs, nano-sized polar clusters made up of frozen soft phonons, acts as an extrinsic polarization mechanism of $\text{Ba}_{0.6}\text{Sr}_{0.4}\text{TiO}_3$ phase. At zero bias field, the dipole moments of PNRs thermally fluctuate between equivalent directions separated by energy barriers. Under bias electric field, PNRs were electrically polarized by the applied bias field. The polarization reorientation of PNRs following the applied bias field was proposed to be an extrinsic contribution to the dielectric nonlinearity [20]. Continuous bias field sweeps are favorable for retaining the polarization freezing state of PNRs. As a result, the extrinsic contribution of PNRs to the dielectric nonlinearity was depressed. The tunability measured in the eighth cycle degraded by about 37% relative to the value of the first cycle (Fig. 9b). The evident degradation of the tunability suggests a substantial contribution of PNRs in $\text{Ba}_{0.6}\text{Sr}_{0.4}\text{TiO}_3$ phase to the dielectric nonlinearity of the composite specimen.

Conclusions

40 wt.% $\text{Ba}_{0.6}\text{Sr}_{0.4}\text{TiO}_3$ -60 wt.% MgO composite ceramics were prepared from $\text{Ba}_{0.6}\text{Sr}_{0.4}\text{TiO}_3$ powder synthesized by citrate method and fine MgO powder. The composite specimens sintered at 1150-1270 °C achieved good densification. The structure and dielectric properties of the specimens were investigated. The results highlight an important role of sintering temperature in modulating the microstructure and dielectric properties of the specimens. Sintering at 1250 °C was determined to be preferred for the composite system in terms of the nonlinear dielectric properties of the specimens under bias electric field. The specimen sintered at this temperature exhibited a dielectric constant (ϵ_r) of 207 and a dielectric loss ($\tan\delta$) of 0.11% at 10 kHz along

with a tunability of 18.5% and a figure of merit (FOM) of 168 at 10 kHz and 30 kV/cm. The nonlinear dielectric properties of the specimen in continuous cycle of bias electric sweep were dependent on field history. The phenomenon was tentatively interpreted in relation to PNRs in $Ba_{0.6}Sr_{0.4}TiO_3$ phase of the composite specimen. It is suggested that the polarization reorientation of PNRs in $Ba_{0.6}Sr_{0.4}TiO_3$ phase under bias electric field substantially contributed to the dielectric nonlinearity of the composite specimen.

Acknowledgments

This work was supported by the National Natural Science Foundation of China (No. 51072146), the Ministry of Education (No. 20100143110006), Hubei Provincial Science and Technology Department (No. 2011CDA057) and Hubei Polytechnic University (No. 12xjz02R). One of the authors (Q. Xu) is grateful to the Human Resources and Social Security Department of Hubei Province (No. 2011-762) for supporting the research.

References

1. L.C. Sengupta and S. Sengupta, *Mater. Res. Innovations* 2 (1999) 278-282.
2. A.K. Tagantsev, V.O. Sherman, K.F. Astafiev, J. Venkatesh and N. Setter, *J. Electroceram.* 11 (2003) 5-66.
3. L.B. Kong, S. Li, T.S. Zhang, J.W. Zhai, F.Y.C. Boey and J. Ma, *Prog. Mater. Sci.* 55 (2010) 840-893.
4. W. Chang and L. Sengupta, *J. Appl. Phys.* 92 (2002) 3941-3946.
5. B. Su and T.W. Button, *J. Appl. Phys.* 95 (2004) 1382-1385.
6. Y. Chen, X.L. Dong, R.H. Liang, J.T. Li and Y.L. Wang, *J. Appl. Phys.* 98 (2005) 064107-1-5.
7. Y. Chen, Y.Y. Zhang, X.L. Dong, G.S. Wang and F. Cao, *J. Am. Ceram. Soc.* 93 (2010) 161-166.
8. X.J. Chou, J.W. Zhai and X. Yao, *Appl. Phys. Lett.* 91 (2007) 122908-1-3.
9. J.J. Zhang, J.W. Zhai, X.J. Chou and X. Yao, *J. Am. Ceram. Soc.* 91 (2008) 3258-3262.
10. J.J. Zhang, J.W. Zhai, H.T. Jiang and X. Yao, *J. Phys. D: Appl. Phys.* 41 (2008) 195405-1-7.
11. S.M. Ke, H.Q. Fan, W. Wang, G.C. Jiao, H.T. Huang and H.L.W. Chan, *Compos. Part A-Appl. S.* 39 (2008) 597-601.
12. T. Hu, H. Jantunen, A. Deleniv, S. Leppavuori and S. Gevorgian, *J. Am. Ceram. Soc.* 87 (2004) 578-583.
13. D. Zhang, W.F. Hu, C. Meggs, B. Su, T. Price, D. Iddles, M.J. Lancaster and T.W. Button, *J. Eur. Ceram. Soc.* 27 (2007) 1047-1051.
14. X.F. Zhang, Q. Xu, Y.H. Huang, H.X. Liu, D.P. Huang and F. Zhang, *Ceram. Int.* 36 (2010) 1405-1409.
15. X.F. Zhang, Q. Xu, H.X. Liu, W. Chen, M. Chen and B.H. Kim, *Physica B* 406 (2011) 1571-1576.
16. S. Agrawal, R. Guo, D. Agrawal and A.S. Bhalla, *Ferroelectrics* 306 (2004) 155-163.
17. A. Feteira, D.C. Sinclair, I.M. Reaney, Y. Somiya and M.T. Lanagan, *J. Am. Ceram. Soc.* 87 (2004) 1082-1087.
18. X.F. Liang, W.B. Wu and Z.Y. Meng, *Mater. Sci. Eng. B* 99 (2003) 366-369.
19. J.J. Zhang, J.W. Zhai, X.J. Chou, J. Shao, X. Lu, X. Yao, *Acta Mater.* 57 (2009) 4491-4499.
20. C. Ang and Z. Yu, *Phys. Rev. B* 69 (2004) 174109-1-8.
21. K.M. Johnson, *J. Appl. Phys.* 33 (1962) 2826-2831.
22. J.W. Liou and B.S. Chiou, *Jpn. J. Appl. Phys.* 36 (1997) 4359-4368.
23. K.F. Astafiev, V.O. Sherman, A.K. Tagantsev and N. Setter, *J. Eur. Ceram. Soc.* 23 (2003) 2381-2386.
24. J.W. Liou and B.S. Chiou, *J. Am. Ceram. Soc.* 80 (1997) 3093-3099.